BULLETIN
DE
L'ACADÉMIE POLONAISE DES SCIENCES

Rédacteur en chef
K. KURATOWSKI

Rédacteur en chef suppléant
S. KULCZYŃSKI

CLASSE TROISIÈME

Rédacteur de la Série
L. INFELD

Comité de Rédaction de la Série
K. BORSUK, S. LESZCZYCKI, J. SAMSONOWICZ, M. ŚMIAŁOWSKI

VOLUME II
NUMÉRO 6

VARSOVIE 1954

PRINTED IN POLAND

PAŃSTWOWE WYDAWNICTWO NAUKOWE — WARSZAWA 1954

Nakład 1019 + 100 egz.	*Rękopis dostarczono 11. V. 1954*
Ark. wyd. 3·0, druk. $2^{14}/_{16}$	*Podpisano do druku 14. VII. 1954*
Papier bezdrzewny sat. 80 g kl. III	*Druk ukończono 17. VII. 1954*
Format B5, 70×100 cm	*Zam. prod. 263/54 Cena zł 5,—*

KRAKOWSKA DRUKARNIA NAUKOWA, KRAKÓW, UL. CZAPSKICH 4

BULLETIN DE L'ACADÉMIE
POLONAISE DES SCIENCES
Cl. III — Vol. II, No. 6, 1954

MATHEMATICS

Rational Functions Univalent on Sets Separating the Plane

by

A. PLIŚ

Communicated by K. KURATOWSKI on March 30, 1954

Let us suppose that the system of $n+1$ integers $k_0, \ldots, k_n$ fulfils the following conditions:

$$k_0 + \ldots + k_n = 0, \tag{1}$$

$$k_j \neq 0 \qquad \text{for} \quad 0 \leqslant j \leqslant n, \tag{2}$$

$$|k_0| + \ldots + |k_n| \leqslant 2n, \tag{3}$$

and the points $p_0, \ldots, p_n$ of the plane of complex numbers are distinct. K. Kuratowski proved ([1], Théorème II) that under these assumptions there exists a curve A separating the plane between every pair of points p_i, p_j $(i \neq j)$ and a function which is univalent on A and homotopic to the rational function

$$r(z) = (z - p_0)^{k_0} \ldots (z - p_n)^{k_n}. \tag{4}$$

In connexion with this theorem he put the question, *whether there exists a curve B separating the plane between every pair of points p_i, p_j $(i \neq j)$ and on which the function* (4) *is univalent.* The answer to this question is *negative.* We shall give an example of a function of the form (4) which satisfies conditions (1)—(3) and is not univalent on any curve B having the above mentioned property.

It is evident that the function

$$r_0(z) = z^2 - \frac{1}{z^2} = z^{-2}(z-1)(z+1)(z-i)(z+i)(z-\infty)^{-2}, \qquad (z - \infty = 1)$$

fulfils conditions (1)—(3). Let us suppose that on a certain curve B separating the plane between every pair of points $1, -1, i, -i, 0, \infty$, and in particular between the points $0, \infty$, the function $r_0(z)$ is univalent.

Since the function $\bar{r}(z) = z^2 = z^2(z - \infty)^{-2}$ satisfies (1), (2) and does not fulfil condition (3) (where $n = 1$, $p_0 = 0$, $p_1 = \infty$), there exist (see [1], Théorème I, and [2], p. 10) on B two distinct points z_1, z_2 such that $z_1^2 = z_2^2$.

Hence we have

$$r_0(z_1) = z_1^2 - \frac{1}{z_1^2} = z_2^2 - \frac{1}{z_2^2} = r_0(z_2),$$

and therefore the function $r_0(z)$ is not univalent on B.

This contradiction with our assumption completes the proof.

Institute of Mathematics, Polish Academy of Sciences

REFERENCES

[1] Kuratowski K., *Fonctions rationnelles qui sont homotopes à des fonctions biunivoques sur certains sous-ensembles du plan,* Fund. Math. **41** (1954).

[2] — *Sur une propriété analytique des homéomorphies définies sur des continus plans,* Bull. Acad. Polon. Sci., Cl. III, **2** (1954), 9.

BULLETIN DE L'ACADÉMIE
POLONAISE DES SCIENCES
Cl. III — Vol. II, No. 6, 1954

MATHEMATICS

Antoine Phenomena and Geometric Properties of Simple Arcs

by

A. KIRKOR

Presented by K. BORSUK on April 2, 1954

A simple arc J lying in the Euclidean 3-space E_3 will be said to be *wildly imbedded* in E_3 [1] if there is no homeomorphism of E_3 onto itself mapping J onto a rectilinear segment. In particular, every *Antoine arc* is wildly imbedded, i. e. every simple arc $J \subset E_3$ containing a perfect 0-dimensional subset A whose complement $E_3 - A$ is not simply connected. A perfect 0-dimensional set $A \subset E_3$ having this last property will be called an *Antoine set.*

There exist examples [1] of wildly imbedded arcs containing no Antoine set. The question arises: what geometric properties are implied by the fact that an arc is wildly imbedded? A result which helps to answer this question was established by J. W. Milnor [2], who proved that a simple arc cannot be wildly imbedded if it has everywhere an oriented tangent, continuously depending on the point of contact. But certain examples given by R. H. Fox and E. Artin [1] show that a simple arc can be wildly imbedded when it fails to have a continuously oriented tangent in at least one point. Moreover K. Borsuk has observed that there exist wildly imbedded arcs having everywhere an unoriented tangent depending continuously on the point of contact. An example of this kind can be obtained by a simple modification of an example of a wildly imbedded arc J, due to Fox and Artin ([1], p. 983, example 1,2) being locally tamely imbedded everywhere, the end-point a excepted. One can easily see that J can be constructed in such a manner that $a = (0,0,0)$ and that $J - (a)$ lies in the open set G defined by the inequalities:

$$x^2 + y^2 < z^4, \; z > 0.$$

Moreover we can assume that $J - (a) = \sum_{n=1}^{\infty} J_n$, where $J_1, J_2, \ldots, J_n, \ldots$ are simple arcs with disjoint interiors and diameters convergent to 0 and such that

1. J_n has the point a_n as origin and a_{n+1} — as end-point.

2. J_n has everywhere an oriented tangent $T_{n,p}$ continuously depending on the point of contact p.

3. If $\alpha_n(p)$ denotes the angle between $T_{n,p}$ and the z-axis, then $|\sin \alpha_n(p)| < \frac{1}{n}$.

4. $T_{n,a_{n+1}}$ and $T_{n+1,a_{n+1}}$ differ at most by the orientation.

It can easily be seen that the arc $J = \sum_{n=1}^{\infty} J_n + (a)$ obtained in this manner has everywhere an unoriented tangent (also at the end-point a) and that this tangent depends continuously on the point of contact.

J is not an Antoine arc. To show this, let us introduce the following definition: a point p of a closed set $F \subset E_3$ will be said to be a *linking point*, if every neighbourhood of p contains a closed path not null-homotopic in $E_3 - F$. By a *net Antoine set* we understand an Antoine set, each of whose points is a linking point. It is easy to show that the set of all linking points of an Antoine set is always a net Antoine set. Obviously no point $p \in J - (a)$ is a linking point of J and hence J is no Antoine arc.

It is easy to see that the paratingent (in the sense of G. Bouligand [3], p. 72) must contain all the directions of E_3 at any linking point of an Antoine set. And using some results of G. Choquet ([4] p. 192), concerning the set of points in which the contingent of a perfect set is identical with the paratingent, we infer that if A is a net Antoine set lying on a simple arc L, then the set of points of A at which L has the unoriented tangent is of the first category on A (in the sense of R. Baire). Consequently every Antoine arc contains an uncountable set of points at which there is no tangent (even unoriented).

It follows that the geometric properties of an Antoine arc cannot be quite regular and the question arises whether such an arc may be rectifiable. First, let us prove that the classical construction, due to L. Antoine [5], leads to arcs of infinite length.

Let $A_1 = T_1$ be a solid torus and let $T_{1,1}, \ldots, T_{1,m_1}$ be the finite set of disjoint tori lying in T_1, similar to T_1 and forming such a chain, that every closed path which is not null-homotopic in $E_3 - T_1$ is also not null-homotopic in $E_3 - \sum_{l=1}^{m_1} T_{1,l}$. Assuming the set $A_k \subset E_3$ to have been defined as the finite sum of tori $T_{k,1}, T_{k,2}, \ldots, T_{k,m_k}$ all of which are similar to T_1, let us denote by $\varphi_{k,l}$ a homothetic mapping throwing T_1 onto $T_{k,l}$ and let

$$A_{k+1} = \sum_{l=1}^{m_k} \varphi_{k,l}(T_{1,1} + \ldots + T_{1,m_1}).$$

The set $A = \prod_{k=1}^{\infty} A_k$ is precisely the set constructed by L. Antoine [5]. It is

easy to prove that the linear measure (in the sense of F. Hausdorff [6]) of the set A is infinite and so is the length of any arc $J \supset A$.

It is easy to show that the linear measure of every Antoine set is > 0. We shall prove that it can be finite and, moreover, that there exist Antoine arcs of finite length.

By a *graph* let us mean a homogeneously 1-dimensional polyhedron P and by its *constituent* — the closure of any component of the set $P - P_0$, where P_0 denotes the set of all ramification points of P. Let $\Omega \subset E_3$ be a circle of radius r and centre o and a, b — any points of Ω such that $\varrho(a,b) < \delta(\Omega)$. If $a \neq b$, we denote by $C = C(a,b)$ the shorter of two arcs cut out of Ω by a and b. If $a = b$, we put $C(a,b) = \Omega$. By $w = w(a,b)$ we denote such a point of $C - (a) - (b)$ that the arcs $C(a,w)$ and $C(w,b)$ are congruent. For every positive $\varkappa < 1/12\,\delta(C)$ let us denote by w' the point

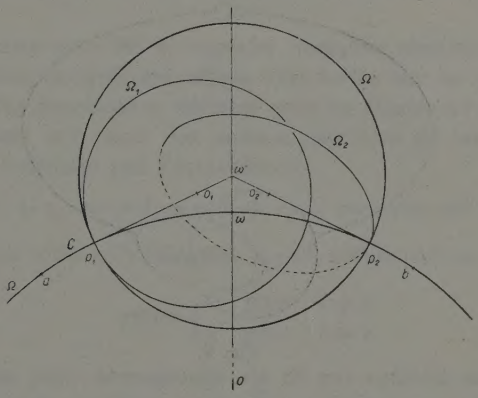

Fig. 1. Ω' denotes the intersection of S_2 with the plane of

of the ray $\overrightarrow{ow}$ lying at the distance $(r^2 + \varkappa^2)^{1/2}$ from o. Let $Q_{C,\varkappa}$ denote the ball $\underset{p}{E}[\varrho(p,w') \leqslant \varkappa]$, S_2 — its boundary and $p_i, i = 1,2$, the points of intersection of S_2 with C. Let o_i be the point lying on the segment $\overline{p_i w'}$ at the distance $\varkappa/4$ from w', Ω_1 — the circle with centre o_1, passing through the point p_1 and lying in the plane of Ω, and Ω_2 — the circle with centre o_2, passing through the point p_2 and lying in the plane perpendicular to the plane of Ω. Evidently the circles Ω_1 and Ω_2 are linked. Putting

$$\eta_\varkappa(C) = C - Q_{C,\varkappa} + \Omega_1 + \Omega_2$$

we define an elementary operation $\eta_\varkappa(C)$ for every circular arc (see Fig. 1).

Now we can define by induction two sequences of compact sets $\{A_n\}$ and $\{A_n^*\}$ in the following way: let $A_0 \subset E_3$ be a circle and A_0^* the closed spherical neighbourhood of A_0 with the radius

$$\varrho_0 < \tfrac{1}{2}\,\delta(A_0).$$

Choose a point $a_0 = b_0 \in A_0$ and let $C_1^{(0)} = C(a_0, b_0) = A_0$. Suppose now that the graph A_n and its closed spherical neighbourhood A_n^* are already defined for some $n \geqslant 0$. Moreover, let us suppose that every one of the constituents $C_1^{(n)}, C_2^{(n)}, \ldots, C_{k_n}^{(n)}$ of A_n is a circular arc and that every circle $\subset A_n$ contains at least one ramification point of A_n. We define the graph A_{n+1} by the formula

$$A_{n+1} = \sum_{i=1}^{k_n} \eta_{\varkappa_{n+1}}(C_i^{(n)}),$$

where the positive number $\varkappa_{n+1}$ is so small that $A_{n+1} \subset \operatorname{Int}(A_n^*)$. The set A_{n+1}^* is defined as a closed spherical neighbourhood of A_{n+1} with radius ϱ_{n+1} so small that $A_{n+1}^* \subset \operatorname{Int}(A_n^*)$ and that A_{n+1} is a deformation retract of A_{n+1}^*. Fig. 2 shows the set A_2.

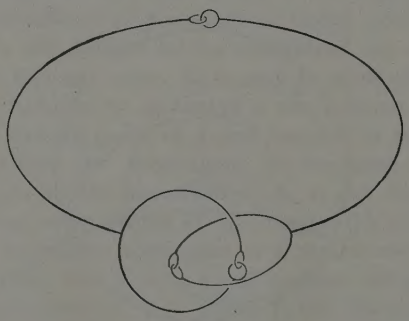

Fig. 2.

It is easy to prove that $A = \prod_{n=0}^{\infty} A_n^*$ is an Antoine set. Choosing the sequence $\{\varkappa_n\}$ so that the series $\sum_{n=0}^{\infty} 2^{3n} \varkappa_n$ converges, we can construct a simple arc of finite length containing the set A and having a continuously oriented tangent almost everywhere in the sense of Baire.

Institute of Mathematics, Polish Academy of Sciences

REFERENCES

[1] Fox R. H. and Artin E., *Some Wild Cells and Spheres in Three-Dimensional Space*, Ann. of Math. **49** (1948), 979.

[2] Milnor J. W., *On the Total Curvature of Knots*, Ann. of Math. **52** (1950), 248.

[3] Bouligand G., *Introduction à la géométrie infinitésimale directe*. Paris, 1932.

[4] Choquet G., *Application des propriétés descriptives de la fonction contingente à la théorie des fonctions de variable réelle et à la géométrie différentielle des variétés cartésiennes*, Journ. de Math. Pures et Appl. **26** (1947), 115.

[5] Antoine L., *L'homéomorphie de deux figures et leurs voisinages*, Journ. de Math. Pures et Appl. **4** (1921), 221.

[6] Hausdorff F., *Dimension und äusseres Mass*, Math. Ann. **79** (1918), 157.

BULLETIN DE L'ACADÉMIE
POLONAISE DES SCIENCES
Cl. III — Vol. II, No. 6, 1954

MATHÉMATIQUE

Sur les produits cartésiens des groupes cycliques infinis

par

A. EHRENFEUCHT et J. ŁOŚ

Présenté par K. KURATOWSKI le 2 Avril 1954

Le but de cette note est de signaler quelques résultats sur les produits cartésiens des groupes cycliques infinis, c'est-à-dire sur les groupes C^T composés de toutes les fonctions x définies pour les éléments t d'un ensemble T et dont les valeurs $x(t)$ sont des entiers, l'addition de ces fonctions étant définie comme d'habitude par l'équivalence:

$$x = x_1 + x_2 \cdot \equiv \cdot [x(t) = x_1(t) + x_2(t), \text{ quel que soit } t \in T].$$

Désignons par $e^{(s)} (s \in T)$ l'élément $x \in C^T$ défini par les formules

$$x(t) = \begin{cases} 0 & \text{pour } t \neq s \\ 1 & \text{pour } t = s \end{cases}$$

et par C^{T^*} le plus petit sous-groupe de C^T qui contient tous les éléments $e^{(s)}$ où $s \in T$. Le groupe C^{T^*} est évidemment un groupe abélien libre; il est dit le produit direct de C^T.

1. Si $\overline{\overline{T}} < \aleph_0$, on a $C^T = C^{T^*}$ et alors les lemmes suivants n'exigent aucune démonstration.

(1.1) *Si $h(C^T) \subset C$ est un homomorphisme (C étant le groupe des nombres entiers), nous n'avons $h(e^{(s)}) \neq 0$ que pour un nombre fini de $s \in T$.*

(1.2) *Si $h_1(C^T) \subset C$ et $h_2(C^T) \subset C$ sont deux homomorphismes tels que $h_1(x) = h_2(x)$ pour $x \in C^{T^*}$, on a $h_1 = h_2$.*

Il paraît intéressant que le lemme (1.1) admet une généralisation valable pour tous les groupes C^T sans aucune restriction sur l'ensemble T, tandis que le lemme (1.2) n'est valable que pour les ensembles T pour lesquels l'ainsi dit "problème généralisé de la mesure" a une réponse négative *). Plus précisément:

Pour que le lemme (1.2) soit valable pour un groupe C^T, il faut et il suffit qu'il n'existe aucune σ-mesure ne s'annulant pas identiquement, ne pre-

*) Dans le cas $\overline{\overline{T}} = \aleph_0$ ces lemmes ont été démontrés par Specker [2].

nant que des valeurs 0 et 1, s'annulant pour les ensembles finis et définis pour chaque sous-ensemble de T.

Les résultats établis par plusieurs mathématiciens, surtout ceux de S. Ulam [1], permettent d'en déduire que le lemme (1.2) est valable au moins pour les ensembles T qui sont de puissance inférieure au premier alef inaccessible *).

Nous ne considérons dans la suite que les groupes C^T pour lesquels le lemme (1.2) est valable.

2. Les théorèmes suivants sont des conséquences des lemmes (1.1) et (1.2):

Théorème 1. *Tout homomorphisme* $h(C^T) \subset C$ *est de la forme*

$$h(x) = \sum_{i=1}^{n} k_i x(t_i) \quad \text{où} \quad x \in C^T,$$

les nombres entiers $k_1, \ldots, k_n$ *et les éléments* $t_1, \ldots, t_n \in T$ *étant fixes.*

Théorème 2. *Il existe pour tout endomorphisme* ε *du groupe* C^T *une matrice aux termes entiers* $\|a_{t,s}\|_{t,s \in T}$, *verticalement finie (c'est-à-dire que pour* t *fixé, on n'a* $a_{t,s} \neq 0$ *que pour un nombre fini des* $s \in T$*) et telle que* $x \in C^T$, $t \in T$ *et* $\varepsilon(x) = x'$ *entraînent*

$$x'(t) = \sum_{s \in T} a_{t,s} x(s).$$

Nous avons, en vertu de théorème 2, le

Théorème 3. *L'anneau des endomorphismes de* C^T *est isomorphe à celui de toutes les matrices* $\|a_{t,s}\|_{t,s \in T}$ *aux termes entiers, verticalement finies (l'addition et la multiplication de ces matrices étant définies comme d'habitude).*

3. Pour un groupe abélien G, soit H_G l'ensemble de tous les homomorphismes $h(G) \subset C$. L'ensemble H_G peut être envisagé comme un sous-groupe de C^G.

Il est facile de vérifier que si $G = C^{T^*}$, H_G est isomorphe à C^T. Le théorème 1 permet d'établir ce

Théorème 4. *Si* $G = C^T$, H_G *est isomorphe à* C^{T^*}.

Le groupe H_G est dit régulier, si $\bigcap_{h \in H_G} h^{-1}(0) = (0)$. Évidemment, pour chaque sous-groupe G de C^T, le groupe H_G est régulier.

Il est facile de construire un groupe G tel que le groupe H_G soit régulier et isomorphe à C^{T^*}, tandis que G n'est pas isomorphe à C^T. Or, on a le théorème suivant:

*) $\aleph_\lambda$ est dit inaccessible si $2^{\mathfrak{m}} < \aleph_\lambda$ et $\sum_{s \in S} \mathfrak{m}_s < \aleph_\lambda$ pour $\mathfrak{m} < \aleph_\lambda$, $\mathfrak{m}_s < \aleph_\lambda$ et $\bar{\bar{S}} < \aleph_\lambda$.

Théorème 5. *Si H_G est régulier et isomorphe à C^T, G est isomorphe à C^{T^*}.*

Ce théorème peut être généralisé de la façon suivante:

Théorème 6. *Si H_G est isomorphe à C^T, G est un produit direct $G = A \times B$, A est isomorphe à C^{T^*} et $H_B = (0)$.*

Les démonstrations des théorèmes 1 – 6 seront publiées dans Fundamenta Mathematicae.

Institut Mathématique de l'Académie Polonaise des Sciences

OUVRAGES CITÉS

[1] Ulam S., Fund. Math. **16** (1930), 140.

[2] Specker E., *Additive Gruppen von Folgen ganzer Zahlen*, Portugaliae Mathematica **9** (1950), 131.

BULLETIN DE L'ACADÉMIE
POLONAISE DES SCIENCES
Cl. III — Vol. II, No. 6, 1954

MATHEMATICS

A Remark on the Cartesian Product of Two Compact Spaces

by

C. RYLL-NARDZEWSKI

Communicated by K. KURATOWSKI at the meeting of April 23, 1954

J. Novák has defined two compact spaces having a non compact Cartesian product (see [1], p. 111, Theorem 4), and M. Katětov proved the compactness of the Cartesian product of any two compact spaces, one of which is bicompact (see [1], p. 111, Theorem 5).

E. Marczewski put the question whether the bicompactness in the Katětov's theorem is necessary.

In this paper I shall prove a theorem more general than Katětov's result. At the same time this theorem answers the above question, because, in the case $m = \aleph_0$, it permits to replace in the Katětov's theorem the bicompactness by the first denumerability axiom of Hausdorff.

Theorem. *If X is a compact space, if the character of every point $x \in X$ is $\leqslant \mathfrak{m}$, and if Y is $\mathfrak{m}$-compact, then $X \times Y$ is compact.*

We say that the character of a point $x \in X$ is $\leqslant \mathfrak{m}$, if there is a family V_x of power $\mathfrak{m}$ of open sets containing x and such that for every neighbourhood W of x there is a $V \in V_x$ contained in W.

A space X is called $\mathfrak{m}$-compact if for any covering of X composed of $\mathfrak{m}$ open sets there is a finite subcovering.

Obviously, the compactness in the ordinary sense is identical with $\aleph_0$-compactness and the bicompactness is equivalent to the $\mathfrak{m}$-compactness for every $\mathfrak{m}$.

Lemma. *If in the Cartesian product $Z = X \times Y$ of two compact spaces the projection on X of every closed subset of Z is closed, then Z is compact.*

Proof of the Lemma. Let $F_1 \supset F_2 \supset \ldots$ be a sequence of non-void closed subsets of Z. It follows from hypotheses that the projections of F_j on X have a common point x_0. Consider the vertical sections:

$$S_j = \{y \mid (x_0, y) \in F_j\}.$$

Since Y is compact, there is a common point y_0 of S_j, whence (x_0, y_0) is a common point of F_j, q. e. d.

Proof of the Theorem. By Lemma, it suffices to prove that the projection P on X of any closed subset F of $X \times Y$ is closed. Let x_0 be an accumulation point of P and let us consider the above defined family $\boldsymbol{V}_{x_0}$.

For every $V \in \boldsymbol{V}_{x_0}$, let us denote by Q_V the closure of the projection on Y of the set $(V \times Y) \cdot F$. It follows from the $\mathfrak{m}$-compactness of Y that there is a common point y_0 of all Q_V. Obviously $(x_0, y_0) \in F'$, whence $x_0 \in P$, q. e. d.

Institute of Mathematics, Polish Academy of Sciences

REFERENCES

[1] Novák J., *On the Cartesian Product of Two Compact Spaces*, Fund. Math. **40** (1953), 106.

BULLETIN DE L'ACADÉMIE
POLONAISE DES SCIENCES
Cl. III — Vol. II, No. 6, 1954

MATHEMATICS

The Fredholm Theory of Linear Equations in Locally Convex Linear Topological Spaces

by

M. ALTMAN

Communicated by S. MAZUR at the meeting of April 28, 1954

In the present note we give an extension of Leżański's theory [1] of linear equations in Banach spaces to locally convex linear topological spaces. We assume that the linear transformation in question is completely continuous*). In order to prove the corresponding theorems we apply a method which consists essentially in a combination of two methods: one due to Leżański and the other to the author [2].

Let X be a fixed linear topological locally convex space and let T be a linear completely continuous transformation of X into X which maps a neighbourhood $\mathfrak{U}$ of 0 into a compact set. Denote by $\overline{X}$ the set of all additive functionals φ defined on X such that $\sup_{x \in \mathfrak{U}} |\varphi(x)| < +\infty$. $\overline{X}$ is a Banach space. Let $\mathfrak{R}$ be a closed linear subspace of the Banach space of all linear transformations of $\overline{X}$ into $\overline{X}$ and let F be a fixed linear functional defined on $\mathfrak{R}$.

Following Leżański [1] we shall suppose that the conditions ($\boldsymbol{K}$) and ($\boldsymbol{F}$) are satisfied:

($\boldsymbol{K}$) The identical mapping I of $\overline{X}$ into $\overline{X}$ belongs to $\mathfrak{R}$.

The transformation $\overline{T}$ (i. e. the adjoint of T)**) defined only on $\overline{X}$ belongs to $\mathfrak{R}$. If $K_1, K_2 \in \mathfrak{R}$, then $K_1 K_2 \in \mathfrak{R}$. If $K \in \mathfrak{R}$ and if $x_0 \in X$ and $\varphi_0 \in \overline{X}$ are fixed, then the linear transformation M defined by the equation

$$M\psi x = K\psi x_0 \cdot \varphi_0 y \quad \text{for} \quad y \in X \quad \text{and} \quad \psi \in \overline{X},$$

also belongs to $\mathfrak{R}$, and

($\boldsymbol{F}$) $$F(M) = KT\varphi_0 x_0.$$

*) For the definitions and notations see [1] and [2].

**) Notice that the adjoint of T has its range in $\overline{X}$ (see [2], p. 203).

Under hypotheses (K) and (F) we shall examine the linear equation

$$x + Tx = y_0, \tag{1}$$

where $y_0 \in X$, and the homogeneous equation

$$x + Tx = 0. \tag{2}$$

It follows from the corresponding results of [2] (see p. 206) that we can deduce the properties of equations (1) and (2) from the behaviour of the adjoint equations

$$\varphi + \overline{T}\varphi = \psi_0, \quad \text{where } \psi_0 \in \Xi, \tag{3}$$

and

$$\varphi + \overline{T}\varphi = 0. \tag{4}$$

We can now successfully apply Leżański's theory to examine the equations (3) and (4). For this purpose we must write the corresponding expressions which appear in the above theory. But, in all these expressions the transformation K should be replaced by the identical mapping I and the transformation T by its adjoint $\overline{T}$.

Following Leżański ([1], p. 250—254), let us set

$$I\begin{pmatrix}\varphi_1,\dots,\varphi_q\\ x_1,\dots,x_q\end{pmatrix} = \begin{vmatrix}\varphi_1 x_1 & \varphi_1 x_2 & \dots & \varphi_1 x_q\\ \varphi_2 x_1 & \varphi_2 x_2 & \dots & \varphi_2 x_q\\ \dots & \dots & \dots & \dots\\ \varphi_q x_1 & \varphi_q x_2 & \dots & \varphi_q x_q\end{vmatrix} \quad \text{for } \begin{matrix} q = 1,2,\dots\\ x_1, x_2, \dots, x_q \in X\\ \varphi_1, \varphi_2, \dots, \varphi_q \in \Xi\end{matrix}$$

$$a_0 = 1, \; a_q = \frac{1}{q!} F_{\varphi_1 y_1} F_{\varphi_2 y_2} \dots F_{\varphi_q y_q}\left\{I\begin{pmatrix}\psi_1,\dots,\psi_q\\ y_1,\dots,y_q\end{pmatrix}\right\}$$

$$A_0 = \overline{T}, \; A_q = a_q \overline{T} - \overline{T} A_{q-1},$$

$$V_q\begin{pmatrix}\varphi_1,\dots,\varphi_p\\ x_1,\dots,x_p\end{pmatrix} = F_{\psi_1 y_1} \dots F_{\psi_q y_q}\left\{I\begin{pmatrix}\varphi_1,\dots,\varphi_p,\ \psi_1,\dots,\psi_q\\ x_1,\dots,x_p,\ y_1,\dots,y_q\end{pmatrix}\right\}$$

$$D_{p,\lambda}\begin{pmatrix}\varphi_1,\dots,\varphi_p\\ x_1,\dots,x_p\end{pmatrix} = (-1)^p \sum_{q=0}^{\infty} \frac{\lambda^q}{q!} V_q\begin{pmatrix}\varphi_1,\dots,\varphi_p\\ x_1,\dots,x_p\end{pmatrix} \tag{5}$$

It follows on an analogous way ([1], p. 253) that series (5) converges for each λ.

Further, let us set $D_p = D_{p,1}$ and $D = D_0 = D_{0,1}$. Hence,

$$D = D_0 = \sum_{q=0}^{\infty} a_q.$$

We need, in addition, to introduce the following notation

$$g_i x = (-1)^i D_p\begin{pmatrix}\varphi_1,\dots,\varphi_p\\ x, x_1,\dots,x_{i-1},x_{i+1},\dots,x_p\end{pmatrix}, \tag{6}$$

where $\varphi_1,\dots,\varphi_p \in \Xi$, $x_1,\dots,x_p \in X$ and p are fixed.

The operation $I+T$ is said to be of order p if $D_p \neq 0$ and $D_r = 0$ for all $r < p$ $(r \geqslant 0)$, where I is now the identical mapping of X into X.

Theorem 1. *If the operation $I+T$ has the order $p > 0$, then the sequence $g_1, \ldots, g_p$ is the basis of the linear space of all φ which are solutions of the homogeneous equation* (4), *i. e. every solution of* (4) *is a linear combination of elements of the basis* ([1], Theorem 1, p. 258).

Theorem 2. *If the operation $I+T$ has the order $p > 0$, then equation* (1) *has a solution if and only if $g_i y_0 = 0$ for $i = 1, \ldots, p$.*

Theorem 3. *Equation* (1) *is solvable for every $y_0 \in X$ if and only if $I+T$ has the order* 0, *i.e. if $D \neq 0$, and then the transformation $x - \frac{1}{D}\sum_{q=0}^{\infty} A_q x$ is converse to the operation $I+T$* ([1], Theorem 3, p. 259).

Theorem 4. *If the operation $I+T$ has the order $p > 0$, then the homogeneous equation* (2) *has exactly p linearly independent solutions.*

Institute of Mathematics, Polish Academy of Sciences

REFERENCES

[1] Leżański T., *The Fredholm Theory of Linear Equation in Banach Spaces*, Studia Math. **13** (1953), 244.

[2] Altman M., *On Linear Functional Equations in Locally Convex Linear Topological Spaces*, Studia Math. **13** (1953), 194.

BULLETIN DE L'ACADÉMIE
POLONAISE DES SCIENCES
Cl. III — Vol. II, No. 6, 1954

THEORETICAL PHYSICS

Optimal Optical Systems

by

R. S. INGARDEN and H. OCHMAN

Communicated by W. RUBINOWICZ at the meeting of February 22, 1954

As early as 1879, Lord Rayleigh [1] raised the question as to whether it was possible to improve the quality of the final diffraction image given by optical instruments by suitable matching of (non-vanishing) geometrical aberrations. In the large class of optical systems investigated by Rayleigh the geometrical aberrations always caused a reduction of the resolving power of the instrument. However, since the investigations carried out by Rayleigh were not exhaustive, the question remained an open one. The results of later investigations into the influence of aberrations on diffraction images [2]—[9] were equally inconclusive. The aim of the present paper is to give:

(i) a more precise formulation of the problem,

(ii) its solution for rotationally symmetrical optical systems consisting of homogeneous and isotropic media.

For the sake of simplicity, we confine ourselves in this note to the scalar theory of light, to objects which are not self luminous (completely coherent light) and to the meridional plane *). Qualitatively the results for the general case are the same.

The working of the optical system may be represented mathematically as a transformation of the amplitude function, $u(x)$, of the object plane into the amplitude function, $U(\xi)$, of the image plane, the transformation being given by a linear integral operator, cf. [10], [11],

$$U(\xi) = \int_{-\infty}^{+\infty} K(x, \xi)\, u(x)\, dx. \tag{1}$$

Here $K(x, \xi)$ depends only on the optical system, and the co-ordinates x, ξ are chosen in such a way as to make linear magnification equal unity **).

*) We suppose also that no losses of light due to reflection and absorption occur in the optical system. This is realized in good approximation in modern instruments with low-reflecting films.

**) All formulae in this paper are given for Seidel variables, cf. [8].

Representing $u(x)$ in the form of a Fourier integral and introducing a new variable of integration $s = x - \xi$, we obtain

$$U(\xi) = \int_{-\infty}^{+\infty} db\, v(b) e^{ib\xi} \int_{-\infty}^{+\infty} K(s+\xi, \xi)\, e^{ibs}\, ds.$$

Denoting

$$R(\xi, b) = \int_{-\infty}^{+\infty} K(s+\xi, \xi)\, e^{ibs}\, ds, \tag{2}$$

we have

$$U(\xi) = \int_{-\infty}^{-\infty} R(\xi, b)\, v(b) e^{ib\xi}\, db.$$

Representing also the left-hand side of (1) in the form of a Fourier integral, we get

$$V(\beta) = \int_{-\infty}^{+\infty} S(b, \beta)\, v(b)\, db, \tag{3}$$

where $V(\beta)$ is the Fourier transform of $v(b)$ and

$$S(b, \beta) = \frac{1}{2\pi} \int_{-\infty}^{+\infty} R(\xi, b) e^{i(b-\beta)\xi}\, d\xi.$$

We call the functions $K(x, \xi)$, $R(\xi, b)$ and $S(b, \beta)$ a *point characteristic*, a *mixed characteristic* and a *frequency characteristic* respectively of the optical system. For problems of optical resolution the function $R(\xi, b)$ is of special interest. If particularly

$$K(x, \xi) = K(x, -\xi) = K(s)\ ^*),$$

we have

$$R(b) = \int_{-\infty}^{+\infty} K(s) e^{ibs}\, ds,$$

$$S(b, \beta) = R(b)\delta(b - \beta), (\delta(x) \text{ — "Dirac function"})$$

and instead of (3)

$$V(\beta) = R(\beta)\, v(\beta).$$

In this case, therefore, the function $R(b)$ determines a reduction of the amplitude of sinusoidal "test-objects" with frequency b. $R(b)$ characterizes explicitly the resolution power of the instrument and for that reason we shall call it also a *resolution characteristic* of the instrument. In the general case this characteristic depends on the image point **), and this corresponds exactly to the real physical situation.

---

*) This form of K may be considered as the first approximation of the general case, cf. [10].

**) And, of course, on the direction through this point in the image plane. Above we consider the meridional (radial) direction only.

If $R(\xi, b) = \text{const}$ (or $K = \text{const}\,\delta(x-\xi)$, $S = \text{const}\,\delta(b-\beta)$),

$$U(\xi) = \text{const}\int_{-\infty}^{+\infty} v(b)\, e^{ib\xi}\, db = \text{const}\int_{-\infty}^{+\infty} \delta(x-\xi)\, u(x)\, dx = \text{const}\, u(\xi)$$

and

$$V(\beta) = \text{const}\int_{-\infty}^{+\infty} \delta(b-\beta)\, v(\beta)\, db = \text{const}\, v(\beta),$$

i. e. the image is exactly similar to the object.

The function $K(x, \xi)$ may be calculated by a generalization of Born's method [8] to arbitrary: order of aberrations, aperture, and amount of aberrations. The result is a series in Bessel functions of the first kind and integral (non-negative) orders. The coefficients in this series are functions of the aberrational coefficients, of the wave length of light, of the linear and angular aperture of the system for a given object distance and of ξ.

Carrying out the integration in (2) we get finally, see [12],

$$(4)\quad R(\xi, b) = \begin{cases} \dfrac{2A}{n_0^2}\, e^{iP(\xi)} \displaystyle\sum_{k=0}^{\infty} [A_k(\xi) + iB_k(\xi)]\, T_k\left(\frac{b}{b_0}\right)\left(1-\frac{b^2}{b_0^2}\right)^{-1/2} & \text{for} \quad |b| < b_0, \\ 0 \quad \text{or} \quad \infty & \text{for} \quad |b| = b_0, \\ 0 & \text{for} \quad |b| > b_0, \end{cases}$$

where $T_k(x) = \cos(k \arccos x)$ are Chebysheff's polynomials of the first kind, A — numerical aperture of the instrument, n_0 — refractive index in the object space, $P(\xi)$ — an unessential for intensities phase difference between image and object (depending on distortion aberrational coefficients), and A_k, B_k — coefficients of the Bessel functions of k-th order in the expansions of the real and imaginary of K, mentioned above. Besides

$$b_0 = \frac{2\pi A}{\lambda},$$

where λ is the wave length of light. We call b_0 the *limiting (amplitudal) resolving power* of the system *).

For an "ideal system" (without geometrical aberrations) one gets cf. [10],

$$R(\xi, b) = \begin{cases} \dfrac{2A}{n_0^2}\, e^{ip(\xi)} \sqrt{1-\left(\dfrac{b}{b_0}\right)^2} & \text{for} \quad |b| \leqslant b_0, \\ 0 & \text{for} \quad |b| > b_0, \end{cases}$$

where $p(\xi)$ is a known function, $p(0) = \dfrac{\pi}{2}$. We see that the ideal system is not the best one from the point of view of the wave theory of light, since it does not represent the object in a perfect manner even for $|b| < b_0$.

*) For intensities the limiting resolving power is twice as great.

An optical system which in the interval $|b| < b_0$ and for given λ, A, n_0, and ξ satisfies the condition

$$R(\xi, b) \equiv \frac{2A}{n_0^2} e^{iP(\xi)} \tag{5}$$

we shall call a system with *uniform meridional resolution* for the image zone $r = |\xi|$ *). It represents in exactly similar manner (but only in meridional planes and for $r = |\xi|$) all objects having no details smaller than $\frac{2\pi}{b_0}$.

From (4) we get as conditions for such a system

$$\begin{aligned} A_0 &= \frac{2}{\pi} \cos q, \qquad B_0 = \frac{2}{\pi} \sin q, \\ A_k &= \frac{2}{\pi} \cos q \int_{-1}^{+1} T_k(x)\,dx = \frac{2}{\pi} \cos q \, \frac{1 + (-1)^k}{1 - k^2}, \quad k = 1, 2, \ldots, \\ B_k &= \frac{2}{\pi} \sin q \, \frac{1 + (-1)^k}{1 - k^2}, \quad k = 1, 2, \ldots \end{aligned} \tag{6}$$

Here $q = p - P$ may be considered as arbitrary, since we are interested in intensities only. As unknowns in equations (6) we may consider the aberrational coefficients and the phase q.

For a small amount **) of aberrations (in comparison to the wave length) equations (6) are linear with respect to aberrational coefficients. Assuming also that the numerical aperture of the instrument is small and considering successively aberrational coefficients of the 3-rd, 5-th, 7-th orders we get the figures in Table I. It follows therefrom that condition (5) may then be satisfied by taking into account aberrational coefficients at least of the 5-th order. For all orders of aberrations a condition for the existence of a solution of (6) is $r \neq 0$. The axial point is, therefore, the singular point of the problem. Since in the third line of Table I the number of unknowns is ten times greater than the number of equations, it may be possible in this approximation to satisfy condition (5) for eleven image zones by a suitable choice of superfluous unknowns (if there are many values of q this number may be reduced to ten).

TABLE I

Order of aberrations	Number of unknowns	Number of equations
3	6	11
3, 5	15	15
3, 5, 7	29	19

*) The condition (5) is fulfilled by (geometrically) ideal instruments with rectangular apertures in directions parallel to the sides of the aperture. Therefore in these systems non-vanishing aberrations always cause diminishing of the quality of the image in these directions, as was proved by Rayleigh in [1].

**) But not necessarily for small aberrational coefficients.

For larger apertures and a greater amount of aberrations the number of equations for a given order of approximation increases and the number of "corrected" image zones decreases. For a greater amount of aberrations, equations (6) are not more linear in aberrational coefficients.

Condition (5) may be weakened as follows:

$$\left|\frac{n_0^2}{2A}\,\varepsilon^{-iP(\xi)}\,R(\xi, b) - 1\right| \leqslant \varepsilon. \tag{7}$$

In virtue of the well-known properties of Chebysheff's polynomials [13] we may put

$$R(\xi, b) = \frac{2A}{n_0^2}\,e^{iP(\xi)}\left\{1 + \frac{1}{2^{k_0-1}}\left(1 - \frac{b^2}{b_0^2}\right)^{-\frac{1}{2}} \sum_{k=k_0}^{\infty} a_k\, T_k\left(\frac{b}{b_0}\right)\right\}, \tag{8}$$

where

$$\frac{1}{2^{k_0-1}} \leqslant \varepsilon < \frac{1}{2^{k_0-2}}, \tag{9}$$

$$|a_k| \leqslant 2^{k-1}. \tag{9 a}$$

Instead of (6) we now get

$$A_k = \begin{cases} A_k|_{\varepsilon=0} & \text{for } k < k_0 \\ A_k|_{\varepsilon=0} + \dfrac{a_k}{2^{k_0-1}} & \text{for } k \geqslant k_0, \end{cases} \tag{10}$$

$$B_k = \begin{cases} B_k|_{\varepsilon=0} & \text{for } k < k_0 \\ B_k|_{\varepsilon=0} + \dfrac{a_k}{2^{k_0-1}} & \text{for } k \geqslant k_0. \end{cases}$$

Since (7) is an inequality, the values of r for which it is satisfied form intervals instead of isolated points, as was the case with condition (5).

Putting e. g. $\varepsilon = 1/10$ we get $k_0 = 5$ and instead of Table I — Table II Taking into account the 5-th (7-th) order aberrations we may satisfy the condition (7) for 4 (16) image zones of finite width (here multivaluesness of q and also inequalities (9 a) may reduce these numbers).

TABLE II

Order of aberrations	Number of unknowns	Number of equations
3	7	11
3, 5	18	15
3, 5, 7	34	19

If for certain ε the intervals for which (7) is satisfied overlap in such a way as to form one interval covering the whole field of view of the instrument, we say that the *meridional quality* of the image is $1/\varepsilon$. It is possible to define analogously the *tangential quality* $1/\eta$ (i. e. in sections tangential to zones $r = \text{const.}$). We call the product of the meridional and tangentional qualities the *optical quality* of the system, and we call an optical instrument an optimal one in which

the optical quality has a maximum for a given wave length, aperture, focal length, field of view and distance of the object. If $\varepsilon = \eta$, an optimal optical system may be called universal, since it represents in the best possible manner an arbitrary object.

The authors wish to express their thanks to H. Wojewoda, M. Gaj and S. Miękisz (members of the Geometrical Optics Section), for help in calculations.

Institute of Mathematics, Polish Academy of Sciences

REFERENCES

[1] Rayleigh, Phil. Mag. **8** (1879), 261; Sc. Papers, I, Cambridge, 1899 p. 415.
[2] Strehl K., *Theorie des Fernrohrs auf Grund der Beugung des Lichtes*, I, Leipzig, 1894.
[3] Straubel R., Abh. d. Bayr. Akad. d. Wiss., I Abt. **18** (1893), 113.
[4] Wilsing J., Publ. d. Astrophys. Obs. Potsdam **15** (1903), 4, Nr. 48.
[5] Richter R., Z. f. Instrumentenkunde **45** (1925), 1.
[6] Steward G. C., Phil. Trans. Roy. Soc. **A 225** (1925), 131.
[7] Picht J., *Optische Abbildung*, Braunschweig, 1931.
[8] Born M., *Optik*, Berlin, 1933, § 56, p. 195, Berichtigungen.
[9] Nijboer B. R. A., *The Diffraction Theory of Aberrations*, Groningen, 1942.
[10] Mandelstam L., *Weber-Festschrift*, 1912 or *Polnoye sobranie trudov*, I Moscow (1947), p. 229.
[11] — J. Exp. Theor. Ph. **16** (1946), 302 or *Polnoye sobranie trudov*, II Moscow (1948), p. 388.
[12] Watson G. N., *A Treatise on the Theory of Bessel Functions*, Cambridge, 1944, p. 405.
[13] Natanson N. N., *Konstruktivnaya teoria funktsyi*, Moscow, 1949.

BULLETIN DE L'ACADÉMIE
POLONAISE DES SCIENCES
Cl. III — Vol. II, No. 6, 1954

CHEMISTRY

Crystal Structure of Titanium Arsenide, TiAs

by

K. ŁUKASZEWICZ and W. TRZEBIATOWSKI

Communicated by W. TRZEBIATOWSKI at the meeting of February 22, 1954

Preliminary investigations have shown that the titanium arsenide, TiAs, crystallises in the hexagonal lattice and that the unit cell ($a = 3.63_5$, $c = 12.04_0\ kX$) contains 4 molecules of TiAs [1]. In consequence of the reflexions observed, the three following space groups were proposed:

$$D_{6h}^4 - C6/mmc, \qquad C_{6v}^4 - C6mc, \qquad D_{3h}^4 - C\bar{6}2c.$$

If an ordered distribution of atoms is assumed, then $D_{6h}^4 - C6/mmc$ may be accepted, because $C_{6v}^4 - C6mc$ has only two, six and twelvefold positions and $D_{3h}^4 - C\bar{6}2c$ leads to an identical structure if the existing two and fourfold positions only are considered. The space group $D_{6h}^4 - C6/mmc$ offers different possibilities as regards the location of the 4 titanium and 4 arsenic atoms, but a detailed, geometrical analysis and a comparison of the observed and calculated intensities establish the following positions:

Ti:	1/3, 2/3, z	2/3, 1/3, $-z$	1/3, 2/3, $1/2 - z$,	2/3, 1/3, $1/2 + z$
As:	0, 0, 0,	0, 0, 1/2	2/3, 1/3, 1/4	1/3, 2/3, 3/4.

The parameter z of titanium atoms was accepted as being approximately 0.125.

The intensities of reflexions obtained by powder methods with filtrated copper radiation were calculated according to the formula:

$$I_{hkl} = K \cdot L \frac{1 + \cos^2 2\Theta}{\sin^2 \Theta \cos \Theta} F_{hkl}^2,$$

$$F_{hkl} = \sum_{i=1}^{N} f_i \cos 2\pi (hx_i + ky_i + lz_i).$$

Atomic scattering factors in accordance with "*Internationale Tabellen*" [2] were accepted. The absorption coefficient was neglected because the sample formed a thin layer on a glass rod of 0.2 mm. diameter.

TABLE I

Calculated and observed intensities of powder diagram reflexions Cu Kα radiation

h	k	i	l	$\sin^2\Theta\cdot10^4$ calc.	$\sin^2\Theta\cdot10^4$ obs.	I calc.	I obs.	h	k	i	l	$\sin^2\Theta\cdot10^4$ calc.	$\sin^2\Theta\cdot10^4$ obs.	I calc.	I obs.
0	0	0	2	163	—	1.2	—	2	0	$\bar{2}$	9	5687	—	0.7	—
1	0	$\bar{1}$	0	596	—	0.6	—	1	1	$\bar{2}$	10	5865	—	0.8	—
1	0	1	1	637	—	1.1	—	0	0	0	12	5869	—	0.4	—
0	0	0	4	652	—	5.6	—	3	0	$\bar{3}$	4	6019	—	1.2	—
1	0	$\bar{1}$	2	759	760	93.8	*vs*	2	1	$\bar{3}$	7	6171	—	0.04	—
1	0	$\bar{1}$	3	963	965	100.0	*vs*	2	0	$\bar{2}$	10	6461	6463	2.6	*vw*
1	0	$\bar{1}$	4	1248	1246	26.1	*m*	1	0	$\bar{1}$	12	6466		1.8	
0	0	0	6	1467	—	0.5	—	2	1	$\bar{3}$	8	6783	—	0.006	—
1	0	$\bar{1}$	5	1615	1611	27.3	*m*	3	0	$\bar{3}$	6	6834	—	0.3	—
1	1	$\bar{2}$	0	1789	1783	62.7	*s*	2	2	$\bar{4}$	0	7156	7162	9.9	*w*
1	1	$\bar{2}$	2	1952	—	0.2	—	2	0	$\bar{2}$	11	7317	7330	7.0	*vw*
1	0	$\bar{1}$	6	2064	2065	27.2	*ms*	2	2	$\bar{4}$	2	7319		0.04	
2	0	$\bar{2}$	0	2385	—	0.05	—	2	1	$\bar{3}$	9	7476	7498	1.3	*vw*
2	0	$\bar{2}$	1	2426	2442	0.2	*vw*	1	0	$\bar{1}$	13	7485		1.7	
1	1	$\bar{2}$	4	2441		4.4		1	1	$\bar{2}$	12	7658	—	2.3	—
2	0	$\bar{2}$	2	2548	2558	13.1	*w*	3	1	$\bar{4}$	0	7752	—	0.03	—
1	0	$\bar{1}$	7	2595	2617	0.1	*vw*	3	1	$\bar{4}$	1	7793	—	0.1	—
0	0	0	8	2609		9.9		2	2	$\bar{4}$	4	7808	—	1.5	—
2	0	$\bar{2}$	3	2752	2761	16.8	*m*	3	1	$\bar{4}$	2	7915	7917	8.8	*vw*
2	0	$\bar{2}$	4	3037	3043	5.5	*vw*	3	0	$\bar{3}$	8	7975	7981	20.5	*ms*
1	0	$\bar{1}$	8	3205	—	0.01	—	0	0	0	14	7989		0.3	
1	1	$\bar{2}$	6	3256	—	0.7	—	3	1	$\bar{4}$	3	8119	8119	13.1	*w*
2	0	$\bar{2}$	5	3404	3405	7.3	*w*	2	1	$\bar{3}$	10	8250	8257	14.7	*w*
2	0	$\bar{2}$	6	3853	3848	9.7	*wm*	2	0	$\bar{2}$	12	8255		2.1	
1	0	$\bar{1}$	9	3898	—	1.0	—	3	1	$\bar{4}$	4	8404	8403	5.6	*vw*
0	0	0	10	4076	—	0.2	—	1	0	$\bar{1}$	14	8585	8599	9.6	*vw*
2	1	$\bar{3}$	0	4174	—	0.04	—	2	2	$\bar{4}$	6	8623	—	0.4	—
2	1	$\bar{3}$	1	4215	—	0.1	—	3	1	$\bar{4}$	5	8771	8774	10.2	*vw*
2	1	$\bar{3}$	2	4337	4331	10.7	*vw*	2	1	$\bar{3}$	11	9106	9113	22.8	*m*
2	0	$\bar{2}$	7	4382	4402	0.04	*ms*	3	1	$\bar{4}$	6	9219	9217	19.8	*wm*
1	1	$\bar{2}$	8	4397		24.8		2	0	$\bar{2}$	13	9274	—	3.0	—
2	1	$\bar{3}$	3	4541	4542	14.7	*m*	3	0	$\bar{3}$	10	9443	—	1.7	—
1	0	$\bar{1}$	10	4672	4678	3.2	*vw*	4	0	$\bar{4}$	0	9541	—	0.02	—
2	1	$\bar{3}$	4	4826	4824	5.4	*vw*	4	0	$\bar{4}$	1	9582	—	0.2	—
2	0	$\bar{2}$	8	4984	—	0.005	—	4	0	$\bar{4}$	2	9704	9702	11.5	*w*
2	1	$\bar{3}$	5	5193	5189	8.0	*w*	3	1	$\bar{4}$	7	9749	—	0.1	—
3	0	$\bar{3}$	0	5367	5366	10.6	*wm*	2	2	$\bar{4}$	8	9764	9763	58.7	*s*
1	0	$\bar{1}$	11	5528	5531	7.3	*vw*	1	0	$\bar{1}$	15	9767		0.2	
3	0	$\bar{3}$	2	5530		0.04		1	1	$\bar{2}$	14	9778	—	4.6	—
2	1	$\bar{3}$	6	5641	5641	11.4	*w*								

Oscillation diagrams of long exposition time, about [$\bar{1}$ 1 0], [$\bar{1}$ 2 0] and [$\bar{1}$ 3 0], showed also very weak reflexions of the type (0 0 l) and (1 1 l) with $l = 4n + 2$. Therefore, it is evident that the parameter z of the titanium atoms differs slightly from 1/8. The real value of this parameter should be 0.116, as shown by the closest agreement noted between the calculated and observed intensities listed in Table I.

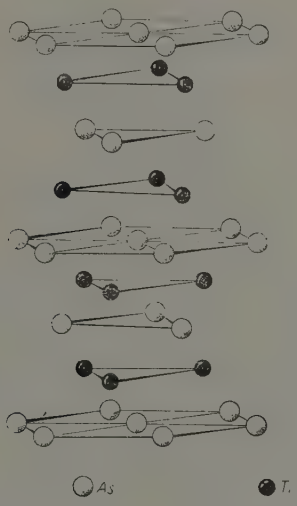

Fig. 1. The hexagonal cell of Ti As

The lattice of Ti As represents a slightly distorted type of close packed layer structure (Fig. 1). There are two different positions of the arsenic atoms. Layers of titanium atoms can be observed alternating with those of arsenic atoms and form a system repeating every 8 layers:

$$AB'CB'AC'BC'A\ldots \begin{matrix} ABC & \text{arsenic layers} \\ B'C' & \text{titanium} \quad \text{„} \end{matrix}$$

The coordination numbers are:

Ti: $3+3$ As: 6

The calculated atomic distances amount to

Ti — 3 As I	2.521 kX
Ti — 3 As II	2.647

Department of Inorganic Chemistry, Institute of Technology, Wrocław

REFERENCES

[1] Trzebiatowski W., Łukaszewicz K., Roczniki Chemii **28** (1954), 150.
[2] *Internationale Tabellen zur Bestimmung d. Kristallstrukturen*, Leipzig, 1935.

BULLETIN DE L'ACADÉMIE
POLONAISE DES SCIENCES
Cl. III — Vol. II, No. 6, 1954

CHEMISTRY

The Anodic Behaviour of Zinc in Phosphoric Acid Solutions

by

J. KAMECKI, Z. ZEMBURA and Z. KUBAS

Communicated by B. KAMIEŃSKI at the meeting of March 15, 1954

Mixtures of solutions of phosphoric acid and its zinc, manganous and ferric salts have for long been applied to the phosphatization of iron, zinc, and other metals [1]. An attempt has been made to shorten the time of phosphatization by applying a direct current (the phosphatized objects being connected as cathodes) or an alternating current [1]. The anodic phosphatization of zinc was carried out in alkaline solutions of phosphates [2]. Independently of this research, solutions of phosphoric acid have found an application in the polishing of metals [3].

Our object in the research here presented was to test the anodic behaviour of zinc, using the same methods as described in previous papers [4], [5]. Samples cut by hand-saw from zinc plates, with a zinc content of 99.993 per cent (the zinc NO corresponding to the norm PN-H-82220) were used for these tests. The plates measured $30 \times 20 \times 10$ mm. After polishing one of the walls (20×30 mm.) of the bloc with emery papers, Nos. 2/0, 3/0, and 4/0, the samples were degreased in benzene and the unpolished surface was paraffined. The active surface therefore measured about 6 cm.^{2} (the dimensions were accurately calculated before each measurement). A sheet of zinc, measuring $65 \times 60 \times 1$ mm., was used as a cathode, hung perpendicularly opposite the anode at a distance of about 4 cm. The measurements were taken in solutions of 43.53, 19.59, 9.83 and 0.927 N H_3PO_4 and also in solutions of 9.83 N H_3PO_4, in which 1.64 and 0.8 gram-equivalents of zinc per litre of phosporic acid had previously been dissolved. The solutions of acid were prepared by diluting concentrated, chemically-pure phosphoric acid (specific gravity 1.7) made by Messrs. "Xenon". A diagram of the apparatus used for measuring is given in Fig. 1, where S denotes the selenium rectifier, R_1, R_2 and R_3 the rheostats, with maximum resistances of 480, 56 and 13 ohms, A the ammeter, V the multi-range voltmeter with resistances of 1500, 6000, and 30,000 ohms, E the saturated calomel electrode, and P the apparatus for measuring the potential by the compensation method.

In the first series of measurements, a check was made of the speed at which the values of the anodic density, and of the tensions and anodic potentials dependent on time were established. The measurements were taken at a point corresponding to the centre of the rising curve, at two points on the "plateau" and at a point lying on the curve of the liberation of oxygen (Figs. 1 and 2). In all cases the time necessary for establishing stationary measurement values was short, not exceeding 3 minutes. For this reason, in further measurements, the tension or density was changed every three minutes. The anodic potentials were measured with reference to a calomel electrode and converted into values with reference to a hydrogen electrode. The results of measuring are given in Figs. 2, 3, 4 and 5.

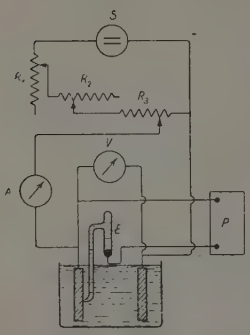

Fig. 1. Diagram of the apparatus used for measurement

The course of the phenomena taking place during the measurements was similar in all cases tested. Initially, the anode dissolved, so that a loose, darkish-grey coating appeared on it. The hydrogen which was given off on the anode as a result of

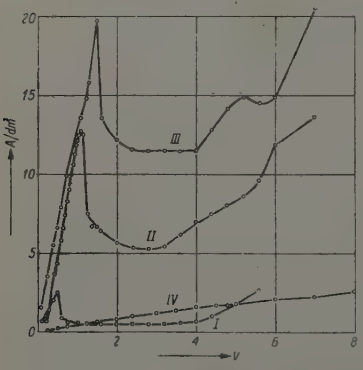

Fig. 2. Curves I, II, III and IV representing the ratio of anodic density to tension of the electrolysis in solutions of 43.53, 19.59, 9.83 and 0.927 N H_3PO_4

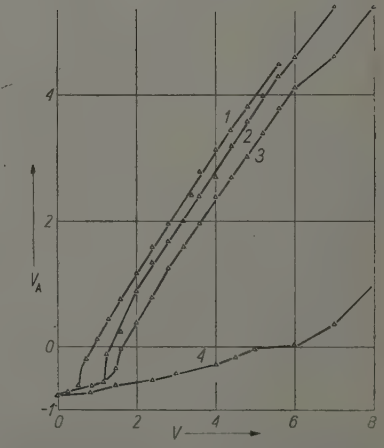

Fig. 3. Curves 1, 2, 3 and 4 representing the ratio of the anodic potential V_A to the tension of the electrolysis in solutions of 43.53, 19.59, 9.83 and 0.927 N H_3PO_4

the direct reaction of the acid with the zinc, ceased to be liberated on the application of sufficiently high tension (cathodic protection) depending on the acid concentration. After the critical tension or density on the anode

had been exceeded, a white coating began to appear irregularly, becoming increasingly uniform as the tension rose. In the third stage of the reaction, that corresponding to the liberation of oxygen, these coatings became increasingly thinner and smoother, and at length disappeared altogether when sufficiently high densities of current were applied.

Attempts at polishing in the region of the plateau (the horizontal section approximately of the density-tension curve) showed that an increase in the coating at some places was accompanied by a smoothing of the metal surface at others. In effect, surfaces partially polished and partially covered with a coating were obtained. In all cases (with the exception of 0.927 N H_3PO_4) good results were obtained above the plateau during the

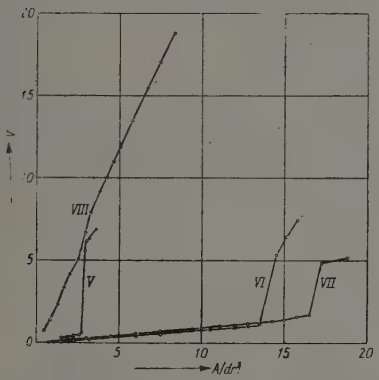

Fig. 4. Curves V, VI, VII and VIII representing the ratio of tension of electrolysis to anodic density in solutions of 43.53, 19.59, 9.83 and 0.927 N H_3PO_4

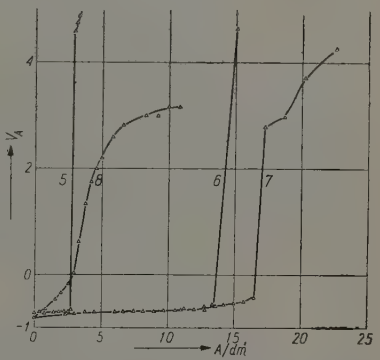

Fig. 5. Curves 5, 6, 7 and 8 representing the ratio of the anodic potential to the anodic density in solutions of 43.53, 19.59, 9.83 and 0.927 N H_3PO_4

period of active liberation of oxygen. The best polishing results were obtained in a solution of 9.83 N H_3PO_4, containing 0.8 gram-equivalents of zinc per litre, when applying a tension of 12—15 V, with a current density of 60 - 80 A/dm.^{2}. The temperature of the bath was about 25° C., and the time taken 3—6 minutes.

Since it is possible during electrolysis for the acid to be neutralized by the zinc, the effect of the zinc salt on the course of electrolysis was investigated. The results are set out in Figs. 6 and 7, in which the curves obtained in a solution of 9.83 N H_3PO_4 are compared with those obtained in a solution of 9.83 N H_3PO_4 in which 1.64 and 0.8 gram-equivalents of zinc per litre of solution have been dissolved.

As seen from the figures, the character of the curves does not undergo any change in spite of the increase in the concentration of zinc salt and the decrease in the concentration of free acid. On the other hand, all critical points, i. e. the level of the plateau, the tension and the critical density, undergo a marked change.

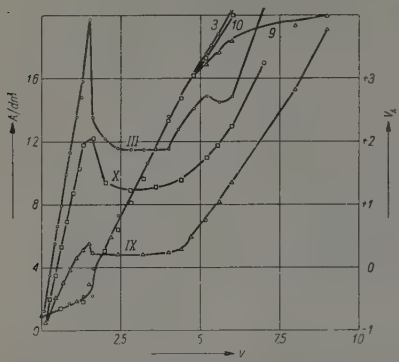

Fig. 6. Curves III, IX and X representing the ratio between the anodic current density and the anodic potential (curves 3.9 and 10) to the tension of the electrolysis V in solutions of 9.83 N H_3PO_4, 9.83 N H_3PO_4 + + 1.6 gram-equivalents of zinc and 9.83 N H_3PO_4 + 0.8 gram-equivalents of zinc per litre

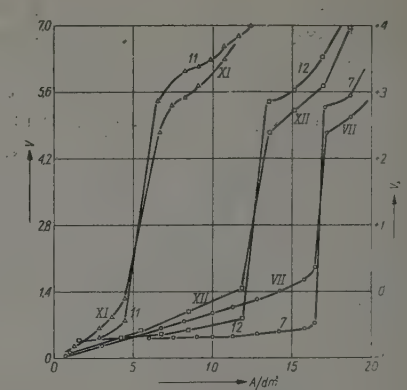

Fig. 7. Curves VII, XI and XII representing the ratio of tension of electrolysis and the anodic potential (curves 7, 11 and 12) to anodic density in solutions as in Fig. 6.

Discussion and results

The curves representing the ratio of tension to anodic density took a similar form in all cases. Initially, the tension rose slowly as the anodic density increased. After exceeding the critical density (for solutions of 43.53. 19.59 and 9.83 N this was 2.9, 13.0 and 16.5 A/dm.² respectively) the increase in the tension was abruptly checked. At the same time there was a sudden jump in the anodic potential (passivity of the anode appeared suddenly).

The curves representing the ratio of anodic density to tension of the electrolysis have a characteristic shape, a fact which has been observed many times before, e. g. in the case of copper in phosphoric acid [3] or of zinc in solutions of KOH [4], [5]. At first the current density in solutions of 43.53, 19.59 and 9.83 N H_3PO_4 increases rapidly (the active state of the anode, of which the potential is near the normal potential of zinc). From the moment when the critical tensions (0.5, 1.15 and 1.5 V respectively) are exceeded, there follows a rapid fall in the anodic density, and at the same time the anodic potential increases by leaps. Then, in spite of increased tension (if we try to keep it at the required level by continual regulation of the resistance of the rheostats) a more or less constant density is maintained (the plateau of the curve).

The lowest point of the plateau depends on the concentration and amounts to 0.5, 5.3 and 11.4 A/dm.² respectively. In this section of the plateau there is a uniform increase in the anodic potential and the tension of

the electrolysis. Oxygen begins to be given off even in the region of the right horizontal end (approximately) of this section of the curve. After the plateau has been passed, an active liberation of oxygen follows, and the current density on the anode remains proportional to the tension applied. Periodic oscillations in the density and tension appeared in the region of the plateau, especially just before the oxygen began to be given off.

The course of the reaction here taking place is probably as follows: in the first phase, when the anodic potential is near the normal potential of zinc (— 0.76 V.), the anode is in the active state and undergoes digestion. As the current density increases, the solution in the neighbourhood of the anode becomes impoverished of $H_2PO_4^-$ ions, and the concentration of Zn^{++} ions increases. This causes an increase in the anodic potential up to the value at which the following reactions become possible: $3\,Zn^{++} + 2\,PO_4^{3-} = Zn_3(PO_4)_2$, $Zn^{++} + 2\,OH^- = Zn(OH)_2$ or $Zn + 2\,OH^- = ZnO + H_2O + 2\,e$ and a white coating is formed on the anode. With a still further increase in tension the anodic potential reaches the value of 1.4 V (which corresponds to the reaction $OH^- = OH + e$). It is possible that the free radical OH [6] causes destruction of the anodic coating. From this moment the active giving off of oxygen on the anode becomes possible.

Department of Physical Chemistry and Electrochemistry,
School of Mining and Metallurgy, Cracow

REFERENCES

[1] Machu W., *Die Phosphatierung*, Verlag Chemie, 1950.
[2] Kamecki J., Romański J., *Prace Instytutu Odlewnictwa*, **3** (1953), 92.
[3] Kamecki J., Zembura Z., Bull. Acad. Polon. Sci. Cl. III, **2** (1954), 31.
[4] — — Bull. Acad. Polon. Sci. Cl. III, **2** (1954), 175.
[5] — — Bull. Acad. Polon. Sci. Cl. III, **2** (1954), 181.
[6] Krasilshchikoff A., Volchkova L., Antonova L., Jurn. fiz. chimii, **27** (1953), 512.

BULLETIN DE L'ACADÉMIE
POLONAISE DES SCIENCES
Cl. III — Vol. II, No. 6, 1954

CHEMISTRY

On the Ternary Positive-Negative Azeotrope: Acetic Acid, Pyridine and *n*-Heptane. XVII

by

K. ZIĘBORAK and M. ZIĘBORAK

Presented by W. ŚWIĘTOSŁAWSKI on March 29, 1954

1. Introductory remarks. In previous papers of this series the composition of ternary positive-negative azeotropes formed by a weak base, a weak acid and a hydrocarbon was discussed [2]. In this paper such an azeotrope, formed by acetic acid (A), pyridine (P), and *n*-heptane (H), is described. Certain details concerning investigations into the binary azeotrope which is composed of acetic acid and pyridine, and also a description of purification, analysis and the technique used in carying out the ebulliometric and other measurements will be given elsewhere [4]. Care was taken to operate with dehydrated substances and their mixtures. As regards the composition of the negative binary azeotrope [(—) A, P], satisfactory agreement was found with Swearingen's experiments [3]. For the binary positive azeotrope (A, H) a boiling temperature of 91.9° C. and an acetic acid concentration of 30.5% were determined.

2. Ebulliometric Method of Measurements. Two Świętosławski ebulliometers [1] were used. The simple one, filled with water, served for measuring pressure changes, the differential one — for measuring the boiling and condensation temperature of the liquid-vapour system under examination. In column I of the Table points are listed corresponding to the composition of the various liquid mixtures examined. They correspond to those shown in Fig. 1 and are selected as being the most characteristic. The thick lines in Fig. 1 show the boiling temperature isobars which were examined. In column II are given the boiling temperatures of the various examined mixtures. The other three columns, III, IV and V, contain the weight percentages of *n*-heptane, acetic acid and pyridine in all the mixtures examined.

The composition of the two binary positive azeotropes (A, H) and (P, H) and of the negative one [(—) A, P] are represented by points C, D and E. On the straight line HC lies point *M*, which corresponds to the minimum

TABLE

Boiling temperatures of mixtures examined

I	II	III	IV	V
H	98.4	100	—	—
P	115.4	—	—	100
A	118.2	—	100	—
C	138.1	—	51.1	48.9
D	91.9	69.5	30.5	—
E	95.46	74.7	—	25.3
Az	96.2	91.5	2.0	6.5
M	96.0	85.87	7.15	6.98
N	98.3	44.4	28.35	27.25
O	95.75	70 7	—	20.3
R	96.5	90	—	10
G_1	96.6	88.44	2.33	9.23
G_2	97.4	70.43	6.93	22.64

boiling temperature of the isobar formed by mixtures of compound H with the binary negative azeotrope [(—) A, H]. The composition of the ternary azeotrope in Fig. 1 a and 1 b is represented by point Az. It lies on the

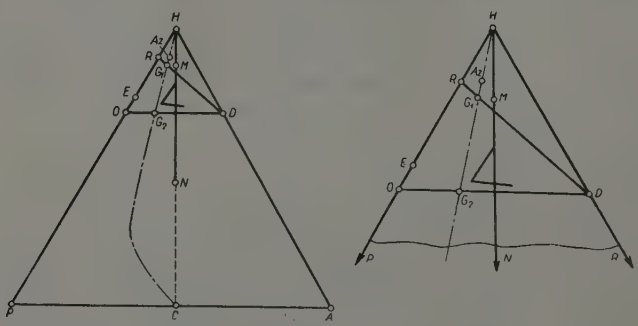

Fig. 1 a and 1 b. Gibbs' Triangle of Concentration (1 a); A, P and H denote pure acetic acid, pyridine and *n*-heptane. Points found inside the Triangle correspond to the mixtures examined and to those listed in the Table. HNC is the main line and H Az G_1 G_2 C — the top-ridge line. The points lying in the vicinity of the composition of the azeotrope are shown in the enlarged drawing 1 b

top-ridge line H Az G_1 G_2 C, which divides the concentration triangle AHP into two portions. All the maximum boiling points, of which the lowest temperature corresponds to that of the mixture having the composition of

a ternary saddle azeotrope, lie on the top-ridge line. In Fig. 2 is presented a tridimensional model of the system examined.

The ternary positive-negative azeotrope is clearly seen to lie in the vicinity of point H, so that the behaviour and composition of this azeotrope differ slightly from that of the almost tangent one [2]. As to the

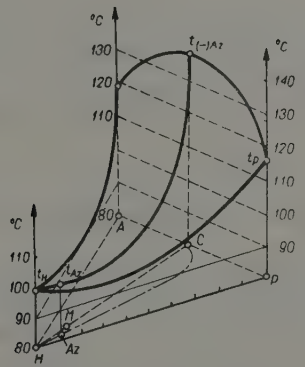

Fig. 2. Tridimensional model of the system composed of acetic acid, pyridine and *n*-heptane. Point M corresponds to the mixture composed of H and azeotrope ((—) A, P), characterized by the minimum boiling temperature; t_{Az} and $t_{(-)A,P}$ are the boiling temperatures of the ternary saddle and the binary negative azeotropes respectively

top-ridge line, it should be emphasised that it lies inside triangle PHC. For this reason, when the shape of the isobar formed from a mixture of H with [(— A, P)] is examined, there appears an "excess" of acetic acid with respect to the saddle ternary azeotrope. Because of this phenomena, considerably increased differences Δt were observed between the boiling and condensation temperatures of the mixtures examined. These phenomena have also been noticed in other similar systems.

We wish to express our thanks to Prof. W. Świętosławski for his help and assistance.

Summary

A ternary positive-negative (saddle) azeotrope formed by *n*-heptane (H), acetic acid (A) and pyridine (P) has been found to exist. The system is composed on one side of a weak acid and a weak base, forming a negative azeotrope belonging, according to Świętosławski's classification, to the second group and, on the other, of a hydrocar-

bon forming binary positive azeotropes with both the acid and the base. The following boiling temperatures and also the compositions of all the four azeotropes have been determined:

[(—) A, P (+) H] + 96.2° C., H% — 91.5%, A% — 2.0, P% — 6.5;
[H, A] + 91.9° C., H% — 69.5, P% — 30.5;
[A, P] + 138.1° C., A% — 51.1%, P% — 48.9%;
[H, P] — 95.6° C., H% — 74.7, P% — 25.3.

In Gibb's concentration triangle the top-ridge line $HAzG_1G_2C$ and the azeotropic point on it Az lie within a triangle HPC, slightly deviating from the main line HNC (Fig. 1).

Department of Physical Chemistry, University of Warsaw

REFERENCES

[1] Świętosławski W., *Ebulliometric Measurements*, Reinhold Publ. Corp., New York, 1945.
[2] — Bull. Acad. Polon. Sci., Cl. III, **1** (1953), 63, 66, 70.
[3] Swearingen E., Ross E., J. Phys. Chem. **31** (1935), 821.
[4] To appear in Roczniki Chem.

BULLETIN DE L'ACADÉMIE
POLONAISE DES SCIENCES
Cl. III — Vol. II, No. 6, 1954

CHEMISTRY

Almost Tangent Azeotropes Formed by Mixing Naphthalene with *m*- and *p*-Cresols. XVIII

by

H. MARKOWSKA-MAJEWSKA

Presented by W. ŚWIĘTOSŁAWSKI on March 29, 1954

1. Previous observations. According to Lecat's tables, naphthalene forms with *m*-cresol an azeotrope containing 5% of naphthalene. Its normal boiling temperature is 0.2° C. lower than that of *m*-cresol itself. The azeotrope formed by *p*-cresol and naphthalene should be considered as a tangent one [2]. The difference in the boiling temperature of these two isomeric cresols is so small that their separation by fractional distillation must be considered as practically impossible [3].

These facts lead to suppose that a mixture of *m*- and *p*-cresols with naphthalene must behave like a single tangent azeotrope. The purpose of this investigation consisted in applying the ebulliometric method to the examination under normal pressure of the shape of the boiling and condensation isobars formed by naphthalene with a cresol fraction boiling at 202° C.

It seemed essential for a better understanding of the phenomena taking place in the course of the distillation of carbolic and middle oils to examine the shape of the boiling temperature isobar by means of the ebulliometric method [1], which enables the boiling temperature of the liquid phase and the condensation temperature of the vapour phase to be measured. A description of the purification of the initial substances and also of the apparatus used will be published elsewhere [6].

2. Experimental Results. In the Table below are given the figures obtained by introducing naphthalene to the fraction of a mixture of *m*- and *p*-cresols boiling at 202° C. In columns I and II the changes in the boiling (t_b) and condensation temperatures (t_c) are listed. The boiling temperature of the cresol fraction was taken as 0.00°. In columns III and IV the differences $t_b - t_c = \Delta t$ and the percentages of naphthalene in the mixture are given.

It can be clearly seen that the shape of the isobar is very flat. For this reason the presence of 28.2% of naphthalene produces an increase in the boiling temperature of 0.66° C. The difference is too small to allow of any separation of naphthalene from the cresol fraction.

TABLE

I	II	III	IV
0.00	— 0 20	0.20	0
+ 0.005	— 0.14	0.14	0.5
+ 0.002	— 0.19	0.19	1.5
— 0.005	— 0.10	0.10	2.2
0.00	— 0.08	0.08	3.0
— 0.007	— 0.08	0.07	3.5
+ 0.007	— 0.08	0.09	4.4
+ 0.01	— 0.05	0.06	5.3
+ 0.02	— 0.05	0.07	5.8
+ 0.03	— 0.03	0.06	6.6
0.03	— 0.01	0.04	7.1
0.05	— 0.03	0.08	7.7
0.06	— 0.01	0.07	8.3
0.07	+ 0.03	0.04	9.5
0.07	— 0.03	0.04	10.2
0.09	— 0.01	0.10	11.2
0.11	+ 0.02	0.09	12.2
0.13	+ 0.07	0.06	13.0
0.14	+ 0.06	0.08	13.1
0.16	+ 0.05	0.11	14.8
0.66	0.43	0.23	28.2
1.34	0.90	0.44	37.9
1.96	1.39	0.57	45.3
2.52	1.74	0.78	51.0

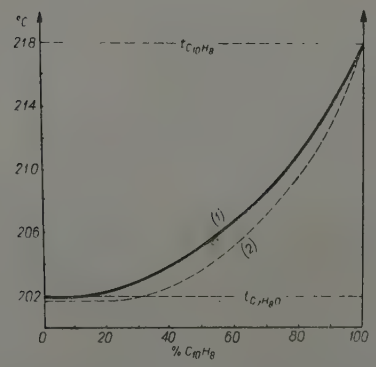

Fig. 1. Boiling (1) and condensation (2) temperature isobars of mixtures of naphthalene and the cresol fraction boiling at 202° C.

Fig. 1 shows the upper part of the isobar, in which the concentration of naphthalene varies from 0% to 100%.

3. Fractional Distillation of a Naphthalene and Cresol Fraction Mixture. To test the results obtained by the ebulliometric method, a fractional distillation was made on a 35-plate distilling column of a mixture containing 25% of naphthalene and 75% of the cresol fraction boiling at 202° C. The distillation curve obtained under atmospheric pressure is given in Fig. 2.

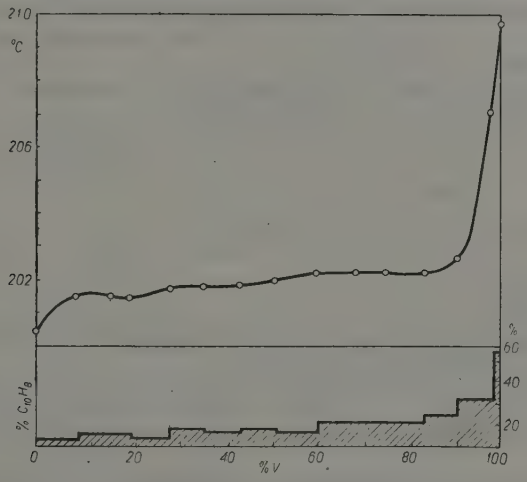

Fig. 2. The distillation curve of a mixture containing 25% naphthalene and 75% cresol fraction

The shape of the curve and analysis of the fraction collected confirmed the conclusions drawn from experimental data obtained by the ebulliometric method. In fact a large amount of naphthalene is entrained with the cresol fraction. It surpassed considerably the amount to be expected on the assumption that an azeotropic composition was to be found in the fractions collected in the receiver.

4. The Lower Limit of the Naphthalene Azeotrope Range with Respect to the Phenol Series. Since the boiling temperature isobar formed by naphthalene and the cresol fraction is tangent to the horizontal line drawn through point t_F, which corresponds to the normal boiling temperature of the cresol fraction, it follows that the lower part of the naphthalene azeotropic range with respect to the phenol series is $218.2 - 202 = 16.2°$ C.

Both Stokowski's [4] experiments and the vapour pressure temperature curves for cresols and naphthalene indicate that under lower pressures than 1 atm. the naphthalene-cresol isobars will be characterized by minimum

boiling temperatures. These minima exist also if the boiling temperature isobar of a naphthalene-cresol mixture is shifted up by the formation of ternary positive-negative azeotrope with a tar base, for instance with a representative of a pyridine series of homologues and their isomers [5].

Summary

1. The boiling temperature isobar of naphthalene with the fraction of *m*- and *p*-cresols boiling practically at a constant temperature of $t_F = 202.0^\circ$ C. was examined.

2. The isobar is tangent to the horizontal line drawn through the point t_F.

3. Świętosławski's differential ebulliometer [1] was used and it was found that for concentrations of up to 5% of naphthalene, the boiling temperature t_F of the cresol fraction remained constant within $\pm 0.010^\circ$ C.

4. A mixture of the cresol fraction with 20—25% of naphthalene cannot be separated even by using a very efficient distilling column.

I wish to express my thanks to Prof. W. Świętosławski for his help and advice.

Institute of General Chemistry, Warsaw

REFERENCES

[1] Świętosławski W., *Ebulliometric Measurements*, Reinhold Publ. Corp., New York 1945; *Ebuliometria*, Warszawa 1935.

[2] Lecat M., *Tables azéotropiques*, Vol. I *Azéotropes binaires orthobares*, Bruxelles 1949.

[3] Goldblum K. B., Mortin B. W., Young R. B., Ind. Eng. Chem. **39** (1947), 1474.

[4] Unpublished results of investigations carried out in the Physicochemical Laboratory, University of Warsaw.

[5] K. Zięborak, H. Markowska-Majewska, Bull. Acad. Polon. Sci., Cl. III, **2** (1954), 343.

[6] To appear in Roczniki Chemii 1954.

BULLETIN DE L'ACADÉMIE
POLONAISE DES SCIENCES
Cl. III — Vol. II, No. 6, 1954

GEOLOGY

Occurrence of Tuffites in the Krosno Beds of the Carpathian Flysch

by

M. KSIĄŻKIEWICZ and T. WIESER

Presented by M. KSIĄŻKIEWICZ on March 9, 1954

At Radziszów, south of Skawina, the Krosno beds form a ridge attaining an altitude of 360 m. Together with the Menilite shales they form a longitudinal belt wedged between two Cretaceous scales.

Within this belt, at a distance of some 1.750 m. west of Radziszów, sandstones and shales of the Krosno beds crop out, dipping southwards. In limeless shales the intercalation of a light, porous rock about 0.5 m. thick is conspicuous. A thick covering of loams prevents us from tracing this rock, but in the neighbouring field, fragments of similar rock are visible. The porous rock splits into plates 1 cm. thick. On its surface tiny flakes of biotite may be observed.

In thin slides it is possible to see that the rock consists of equal amounts of detrital and pyroclastic material. The latter is composed of crystals or crystalline fragments of plagioclase, biotite, predominant volcanic glass and its weathering products.

Plagioclase is characterized by its vitrous, microtynic appearance and columnar features. It occurs in small, whole crystals. Fragments of larger crystals exhibit zoning. Twinning of the albite and carlsbad types is not infrequent. Apatite, liquids, gases and glass are included in the plagioclases, sometimes in the form of negative crystals. The diameter of the grains attains to 0.35 mm., but probably that is not the largest original diameter because of protoclase and sorting in the depositional basin. By measuring the extinction angles in a symmetrical zone the content of anorthite may be determined within the limit 53—54% (acid labradore).

Biotite is another crystalline component of the pyroclastic portion. It has a flaky appearance, with anhedral or subhedral lateral contours. The width of the flakes does not exceed 0.4 mm. Its pleochroism, slightly reduced owing to hydration, is still intensive: X — pale yellow, Y — yellow brown, Z — yellow brown. Apatite is present in biotite and goethite is sometimes also present, forming impregnations along cleavage planes.

Volcanic glass is the most abundant clasmatic component of the rock. Its fragments possess concave and convex contours which are still fairly well preserved. Gas vesicles are visible in glass fragments. As a rule, the isotropic fragments of glass are covered with decomposition products consisting of scaly montmorillonite with birefrigence 0.021 (aluminous montmorillonite). The diameter of the glass grains attains to 0.25 mm.

The detrital portion of the tuffite is composed of quartz sand and silt; some hydromica, glauconite, heavy minerals and argillaceous matter are also present. Detrital quartz is angular on account of the small diameter of its grains, which are mostly of silt dimensions and more rarely of fine-grained sand with a maximal diameter of 0.25 mm. Quartz is probably of metamorphic origin. Rare hydromica occurs in scaly grains which still preserve high birefringence and have a diameter of c. 0.15 mm. Isometric grains of glauconite with aggregate polarisation possess similar dimensions. Among the heavy minerals, zircon is the most abundant. It is associated with rutile, apatite and common hornblende.

The texture of the rock in question is psammitic and vitro-crystalline-clastic. In thin slides the structure shows no apparent orientation; in hand specimens it is porous and parallel.

On the basis of mineralogical analysis of the crystalline portion of the tuffite, it may be concluded that the source material was composed of volcanic dust corresponding to intermediate, presumably dacitic, lavas. This is indicated by the high anorthite content, the zonal structure of the plagioclases, the large quantity of biotite and the lack of sanidine. The large degree of dispersion of pyroclastic components seems to indicate that the eruption was of a paroxysmal character.

It would be interesting to know in which part of the vertical profile of the Krosno beds tuffite occurs. The answer is, however, very difficult, because in the vicinity of Radziszów the Krosno beds do not form a complete series. They are here exceptionally thin (c. 300 m.) and the tuffite occurs approximately in their middle part. Besides, the lower and upper boundaries of the Krosno beds are of a tectonic character in this area.

Except for the tuffs from the upper Cretaceous described by A. Gaweł and M. Książkiewicz [1], no tuffaceous deposits have so far been found in the Flysch zone of the Northern Carpathians. Their presence in the Krosno beds, which belong to the uppermost Eocene and Oligocene, points to the fact that during the period of their deposition there must have been some centres of eruptive activity furnishing volcanic dust which fell into the Flysch sea. There are indications that the extent of the influence of volcanic activity at that period may have been considerable. H. Świdziński ([2] p. 211), describing the Menilite shales of Bukowina in the vicinity of Seletyn, mentions a yellow clay, 1.5 cm. thick, found by Z. Sujkowski to be bentonite. K. Krejci-Graf and W. Wetzel ([3] pp. 83, 92) describe some presumably volcanic admixture in the Oligocene beds of Rumania.

These facts indicate that at a few places far distant from each other (Radziszów, Seletyn in Bukowina, the Trotus valley and the district of Prahova in Rumania) the sediments of the Carpathian Flysch geosyncline received pyroclastic material during the Upper Eocene and Oligocene.

In the internal zone of the Carpathians the period of extensive eruptions commenced between the first and second Mediterranean stages of the Miocene and lasted until the Early Quaternary. But there are several indications that the volcanic activity started earlier. V. Uhlig ([4] p. 894) states that in the Ofen-Kovacs area near Budapest tuffs and fragments of sanidine trachyte occur in the Upper Eocene nummulitic limestones. North of the Matra, ryolitic tuffs lie below the Miocene deposits, and, according to K. Hofman [5] and A. Koch ([6] p. 343), pebbles of trachytic rocks occur in the Mera beds of Transylvania which are of Tongrien age; this proves that before the Middle Oligocene there must have been volcanic eruptions on the inner side of the Carpathian geosyncline.

As there are no indications of any eruptive activity inside the Flysch geosyncline at that time, it may safely be presumed that the volcanic dust occurring in the tuffites of the Krosno beds in the Western Flysch Carpathians derives from the early stage of the Tertiary volcanism of the internal zone.

Institute of Physical Geology, School of Mining and Metallurgy, Cracow

REFERENCES

[1] Gaweł A. and Książkiewicz M., Ann. Soc. Géol. Pol. **12** (1936).
[2] Świdziński H., Bull. Serv. Géol. Pol. **9** (1938).
[3] Krejci-Graf K., Wetzel W., Archiv f. Lagerstättenforschung **62** (1936).
[4] Uhlig V., *Bau und Bild der Karpathen*, Wien, 1903.
[5] Hofman K., Földtani Köziöny, **9** (1879).
[6] Koch A., Mitt. aus dem Jahrb. ungar. geol. Anst. **10** (1894).